Supplementary Information: A j_{eff}=1/2 Kitaev material on the triangular lattice: The case of $NaRuO_2$

Aleksandar Razpopov,[1] David A. S. Kaib,[1] Steffen Backes,[2,3,4] Leon Balents,[5] Stephen D. Wilson,[6] Francesco Ferrari,[1] Kira Riedl,[1] and Roser Valentí[1]

[1] *Institut für Theoretische Physik, Goethe-Universität, 60438 Frankfurt am Main, Germany*
[2] *Research Center for Advanced Science and Technology, University of Tokyo, Komaba, Tokyo 153-8904, Japan*
[3] *Center for Emergent Matter Science, RIKEN, Wako, Saitama 351-0198, Japan*
[4] *CPHT, CNRS, École polytechnique, Institut Polytechnique de Paris, 91120 Palaiseau, France*
[5] *Kavli Institute for Theoretical Physics, University of California, Santa Barbara, California 93106, USA*
[6] *Materials Department, University of California, Santa Barbara, California 93106-5050, USA*

(Dated: May 2, 2023)

Supplementary Note 1: Definition of j_{eff} states

In general, the relativistic basis of d block electrons consists of $j = \{5/2, 3/2\}$ states. However, in an octahedral environment, due to crystal field splitting, the $e_g = \{x^2\text{-}y^2, z^2\}$ orbitals may be high enough in energy, such that a description in terms of $j_{\text{eff}} = \{3/2, 1/2\}$ states is more appropriate [1, 2]. These states are defined by the following combination of $t_{2g} = \{xy, xz, yz\}$ orbitals

$$|1/2, 1/2\rangle_{\text{eff}} = \frac{1}{\sqrt{3}}(-|xy,\uparrow\rangle - i|xz,\downarrow\rangle - |yz,\downarrow\rangle), \quad (1)$$

$$|1/2, -1/2\rangle_{\text{eff}} = \frac{1}{\sqrt{3}}(|xy,\downarrow\rangle + i|xz,\uparrow\rangle - |yz,\uparrow\rangle), \quad (2)$$

$$|3/2, 3/2\rangle_{\text{eff}} = \frac{1}{\sqrt{2}}(-i|xz,\uparrow\rangle - |yz,\uparrow\rangle), \quad (3)$$

$$|3/2, 1/2\rangle_{\text{eff}} = \frac{1}{\sqrt{6}}(-i|xz,\downarrow\rangle - |yz,\downarrow\rangle + 2|xy,\uparrow\rangle), \quad (4)$$

$$|3/2, -1/2\rangle_{\text{eff}} = \frac{1}{\sqrt{6}}(-i|xz,\uparrow\rangle + |yz,\uparrow\rangle + 2|xy,\downarrow\rangle), \quad (5)$$

$$|3/2, -3/2\rangle_{\text{eff}} = \frac{1}{\sqrt{2}}(-i|xz,\downarrow\rangle + |yz,\downarrow\rangle). \quad (6)$$

Supplementary Note 2: Bilinear Hamiltonian in the crystallographic reference frame

In the main text the bilinear Hamiltonian is given in cubic coordinates (shown in Fig. 1b of the main text). Another possible spin coordinate frame, dubbed *crystallographic* frame, is the one in which spin coordinates $(\tilde{S}^x, \tilde{S}^y, \tilde{S}^z)$ co-align with crystallographic (a, b^*, c) directions, as used e.g. in Ref. [3] (and labelled as "cryst" in the following). In the latter framework, focusing on nearest-neighbor bonds, for which anisotropic interactions are relevant, the Hamiltonian

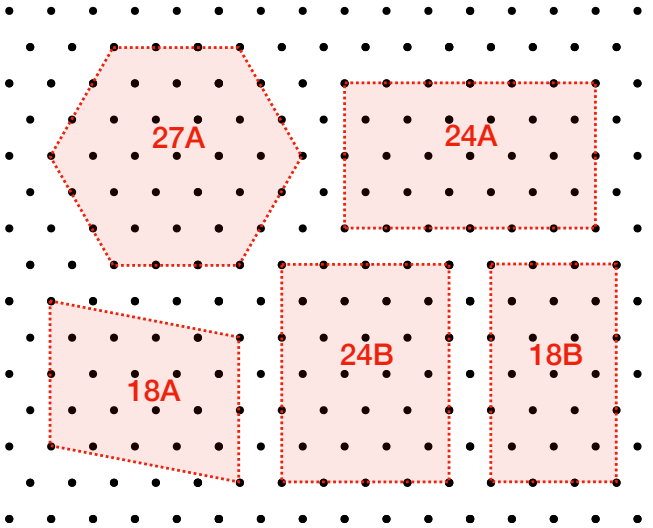

Supplementary Figure 1. **Finite-size clusters used in exact diagonalization calculations.** Dotted lines represent periodic boundaries. Respective number of sites is denoted within each cluster.

reads

$$\begin{aligned}\mathcal{H}_2^{\text{cryst}} = \sum_{\langle i,j\rangle}\{&J^{\text{cryst}}(\tilde{S}_i^x\tilde{S}_j^x + \tilde{S}_i^y\tilde{S}_j^y + \Delta^{\text{cryst}}\tilde{S}_i^z\tilde{S}_j^z)\\ &+ 2J_{\pm,\pm}^{\text{cryst}}[(\tilde{S}_i^x\tilde{S}_j^x - \tilde{S}_i^y\tilde{S}_j^y)c_\alpha - (\tilde{S}_i^x\tilde{S}_j^y + \tilde{S}_i^y\tilde{S}_j^x)s_\alpha]\\ &+ J_{z,\pm}^{\text{cryst}}[(\tilde{S}_i^y\tilde{S}_j^z + \tilde{S}_i^z\tilde{S}_j^y)c_\alpha - (\tilde{S}_i^x\tilde{S}_j^z + \tilde{S}_i^z\tilde{S}_j^x)s_\alpha]\},\end{aligned} \quad (7)$$

where $c_\alpha = \cos(\varphi_\alpha)$, $s_\alpha = \sin(\varphi_\alpha)$ and $\varphi_\alpha = (0, \frac{2\pi}{3}, -\frac{2\pi}{3})$ for X_1-, Y_1- and Z_1-bonds, respectively [3]. In the crystallographic reference frame, the nearest-neighbor couplings of $NaRuO_2$ are $(J^{\text{cryst}}, \Delta^{\text{cryst}}, J_{\pm,\pm}^{\text{cryst}}, J_{z,\pm}^{\text{cryst}}) = (-5.97, -0.39, -2.59, -1.65)$ meV, where we note the unusual negative sign of the XXZ anisotropy parameter Δ^{cryst}.

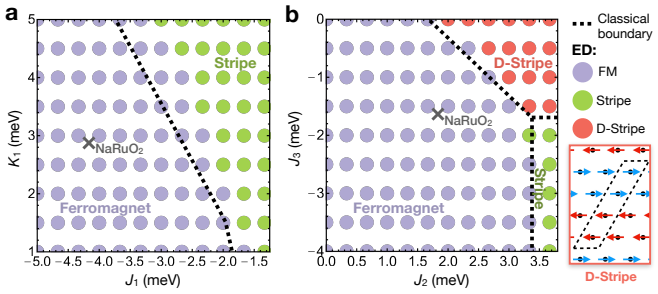

Supplementary Figure 2. **Phases of the magnetic bilinear Hamiltonian around the ab-initio estimate for $NaRuO_2$** Phase diagram of the (in-plane) bilinear Hamiltonian $\mathcal{H}_2$ when tuning **a** the nearest-neighbors interactions J_1 and K_1, **b** the longer-range couplings J_2 and J_3. The remaining parameters are fixed and equal to the ones given in Fig. 1d of the main text. The grey cross indicates the *ab-initio* derived Hamiltonian for $NaRuO_2$. The colored circles show the ground state order obtained by ED calculations (on a coarse finite grid of values, cluster 24A) according to the legend on the right, while the dashed lines mark the classical phase boundaries. The D-Stripe (Double-Stripe) order is depicted on the bottom right of the figure (the magnetic unit cell is marked with dashed lines).

Supplementary Note 3: Details of Exact Diagonalization calculations

In Supplementary Figure 1 we show the various clusters employed in exact diagonalization (ED) calculations. The neutron scattering intensity shown in Fig. 3b of the main text combines results from different momenta allowed on different clusters. For momenta that exist on multiple clusters, the averaged intensity from all such clusters is shown.

Supplementary Note 4: Perturbations to magnetic Hamiltonian

As discussed in the main text, the magnetic Hamiltonian derived in this study yields a ferromagnetic (FM) ordered ground state. However, different experimental samples might have certain variations in their lattice structure [4], changing their magnetic couplings. Furthermore, the *ab-initio* calculation of the magnetic Hamiltonian depends on input parameters and approximations to some degree. It is therefore interesting to consider how stable the FM ground state of the model is against modest perturbations. We here consider for simplicity only our bilinear model $\mathcal{H}_2$ with intra-plane interactions. This precise model is not captured by existing phase diagrams [3, 5] due to the presence of finite Γ', negative Δ^{cryst} (see Supplementary Note 2), and finite further-neighbor J_2, J_3 interactions. We therefore perform various classical energy minimization and ED calculations perturbing around the *ab-initio* derived Hamiltonian. Two phase diagrams are shown in Supplementary Figure 2, in which either K_1 and J_1, or J_2 and J_3, are tuned around the $NaRuO_2$ in-plane bilinear model (marked by the white circle). In all cases, changes of multiple meV to the parameters in the Hamiltonian are needed to destabilize the ferromagnetic state. This amount of variation exceeds the typical degree of uncertainty expected in the *ab-initio* calculations, supporting the assessment of a pristine $NaRuO_2$ compound to be ferromagnetic. Interestingly, we note that a "double-stripe" ("D-Stripe" in Supplementary Figure 2) magnetic order is relatively proximate to the $NaRuO_2$ model. The "double-stripe" order resembles the "stripe" phase, but with a doubled unit cell size, as shown at the bottom right of Supplementary Figure 2.

We also consider slight variations in the U and J_H (Hund's coupling) parameters away from the cRPA-computed values, which are used in the projED derivation for the magnetic Hamiltonians. However, modest variations of these parameters (e.g., ± 0.1 eV for J_H and ± 1 eV for U) still lead to magnetic Hamiltonians with a FM ground state. With decreasing U, the (anisotropic) ring exchange interaction tends to increase, however not enough to destabilize the FM order for realistic U and J_H values.

Supplementary Note 5: Quality of total energy mapping analysis

To quantify the quality of the total energy mapping analysis we consider the difference between the energy of the DFT (GGA+U) calculation and the one provided by the fitting magnetic model. The result is shown in Supplementary Figure 3 for each configuration (labelled by a number). Small deviations between the model calculations and DFT calculations are expected to be accounted for by longer range interactions which are not considered in the model. The small total energy difference (0.049 meV/Ru per configuration) suggests that all relevant exchange couplings are included in the magnetic model.

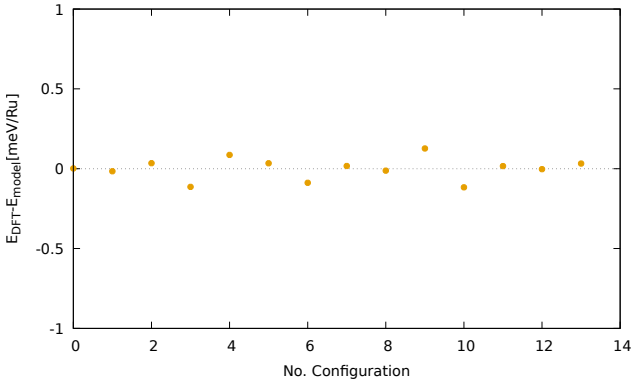

Supplementary Figure 3. **Quality of the total energy mapping analysis.** The difference between the total DFT (GGA+U) energy and the one from the magnetic model is shown as a function of the different magnetic configurations, labelled by an integer number.

[1] B. J. Kim, H. Jin, S. J. Moon, J.-Y. Kim, B.-G. Park, C. S. Leem, J. Yu, T. W. Noh, C. Kim, S.-J. Oh, J.-H. Park, V. Durairaj, G. Cao, and E. Rotenberg, Phys. Rev. Lett. **101**, 076402 (2008).

[2] S. M. Winter, A. A. Tsirlin, M. Daghofer, J. van den Brink, Y. Singh, P. Gegenwart, and R. Valentí, J. Phys. Condens. Matter **29**, 493002 (2017).

[3] P. A. Maksimov, Z. Zhu, S. R. White, and A. L. Chernyshev, Phys. Rev. X **9**, 021017 (2019); Phys. Rev. X **12**, 019902 (2022).

[4] B. R. Ortiz, P. M. Sarte, A. H. Avidor, A. Hay, E. Kenney, A. I. Kolesnikov, D. M. Pajerowski, A. A. Aczel, K. M. Taddei, C. M. Brown, C. Wang, M. J. Graf, R. Seshadri, L. Balents, and S. D. Wilson, Nature Physics (2023), 10.1038/s41567-023-02039-x.

[5] S. Wang, Z. Qi, B. Xi, W. Wang, S.-L. Yu, and J.-X. Li, Phys. Rev. B **103**, 054410 (2021).